An ab Initio Based Global Potential Energy Surface Describing $CH_5^+ \rightarrow CH_3^+ + H_2$†

Zhong Jin, Bastiaan J. Braams, and Joel M. Bowman*

Cherry L. Emerson Center of Scientific Computation and Department of Chemistry, Emory University, Atlanta, Georgia 30322

Received: July 13, 2005; In Final Form: August 24, 2005

A full-dimensional, ab initio based potential energy surface (PES) for CH_5^+, which can describe dissociation is reported. The PES is a precise fit to 36173 coupled-cluster [CCSD(T)] calculations of electronic energies done using an aug-cc-pVTZ basis. The fit uses a polynomial basis that is invariant with respect to permutation of the five H atoms, and thus describes all 120 equivalent minima. The rms fitting error is 78.1 cm^{-1} for the entire data set of energies up to 30 000 cm^{-1} and a normal-mode analysis of CH_5^+ also verifies the accuracy of the fit. Two saddle points have been located on the surface as well and compared with previous theoretical work. The PES dissociates correctly to the fragments $CH_3^+ + H_2$ and the equilibrium geometry and normal-mode analyses of these fragments are also presented. Diffusion Monte Carlo calculations are done for the zero-point energies of CH_5^+ (and some isotopologs) as well as for the separated fragments of CH_5^+, $CH_3^+ + H_2$ and those of CH_4D^+, $CH_3^+ + HD$ and $CH_2D^+ + H_2$. Values of D_0 are reported for these dissociations. A molecular dynamics calculation of CH_4D^+ dissociation at one total energy is also performed to both validate the applicability of the PES for dynamics studies as well as to test a simple classical statistical prediction of the branching ratio of the dissociation products.

I. Introduction

The cation CH_5^+ plays an important role in astrochemistry[1−3] and possibly in combustion chemistry. This cation is also of great basic interest because it is known to be highly fluxional. There have been numerous theoretical studies[4−16] of CH_5^+ since its discovery in mass spectrometry experiments in 1950s.[17] The first detailed insights into CH_5^+ obtained from these calculations were that the minimum, denoted C_s(I), is a C_s structure that is characterized as a "CH_3 tripod" with an "H_2" attached to the carbon. This unusual structure was attributed to three-center two-electron bonding. In addition two saddle points, denoted C_s(II) and C_{2v}, have been characterized. The most accurate calculations[11] report electronic energies of the C_s(II) and C_{2v} saddle points of 33.9 and 286.1 cm^{-1} relative to the global minimum.

The nature of CH_5^+ causes it to be quite resistant to direct experimental characterization. Results from mass spectrometric experiments by Hiraoka and co-workers[18,19] on CH_5^+ are compatible with the 3-center, 2-electron bonded structure of C_s(I) symmetry. However, this experiment is achieved by attaching methane molecules as the thermochemical sensors to the CH_5^+ core. CH_5^+ has complicated IR absorption spectrum. Oka and co-workers recorded the high-resolution infrared spectrum of CH_5^+ in the range of 2750−3150 cm^{-1}. There are approximately 900 spectral lines[20] with considerable spectral congestion and to date these lines have not been assigned. Very recently Asvany et al. reported a low-resolution IR spectrum of CH_5^+ (at 110 K) in the range 0−3500 cm^{-1}.[21] Three broad bands were observed at 1200, 2500, and 3000 cm^{-1}, with nearly continuous absorption in the range 2500−3000 cm^{-1}. The features were captured in a recent classical power spectrum reported by us using a full-dimensional potential energy surface based on MP2/cc-pVTZ calculations.[14] A very similar finding though directly of the IR spectrum via the dipole correlation function using DFT-based direct dynamics was also reported along with this new spectrum.[21]

Theoretically, in addition to the electronic structure calculations, several dynamics studies have been reported. The first dynamical study showing the fluxional nature of CH_5^+ was reported by Marx and Parrinello based on Car−Parrinello dynamics calculations and path-integral simulations.[6,8,9] More recently, we reported the zero point properties of CH_5^+ and isotopologs obtained with classical molecular dynamics and quantum Diffusion Monte Carlo calculations by McCoy[13] and power spectra[14] of CH_5^+ using our semi-global potential energy surface. This PES is a fit to ab initio MP2/cc-pVTZ energies, which is made explicitly invariant with respect to any permutation of the five H atoms. It does describe excitation of CH_5^+ up to fairly high energies; however, it does not describe dissociation. Very recently other semiglobal PES and DMC calculations of the zero-point state were reported, based on CCSD(T)/aug-cc-pVTZ calculations.[15]

For a study of the important interstellar reaction[3]

$$CH_3^+ + HD \rightarrow CH_2D^+ + H_2 \qquad (1)$$

the PES of CH_5^+ must extend to the dissociation limit $CH_3^+ + H_2$. The geometries used in the previous potentials[12−14] were focused in the configuration space around the global minimum of CH_5^+ and so did not describe its dissociation. Motivated by this, we have developed a new potential energy surface that describes dissociation to fragments CH_3^+ and H_2 and present that surface and some calculations with it here.

The surface we describe here is constructed from 36173 CCSD(T) energies obtained with the aug-cc-pVTZ basis set using MOLPRO 2002.6.[22] Section II discusses the details of

* Corrrsponding author. E-mail address: jmbowma@emory.edu.
† Part of the special issue "William Hase Festschrift".

10.1021/jp053848o CCC: $33.50
Published on Web 10/05/2005

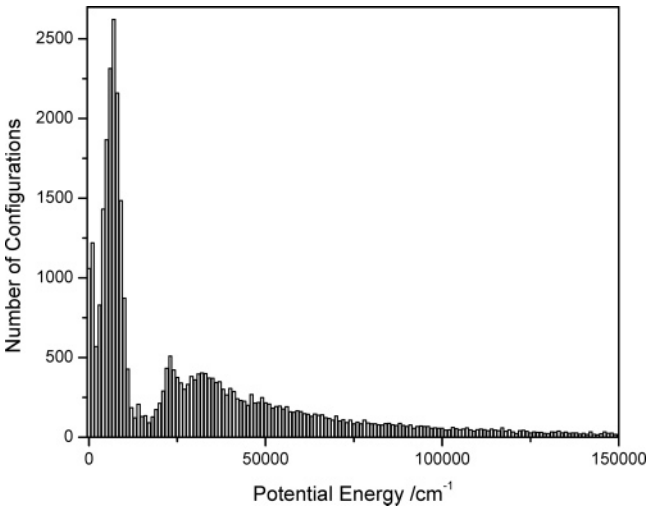

Figure 1. Energy distribution of geometries used in the fit.

the ab initio calculations, the fitting methods as well as tests of the accuracy of the PES in representing the ab initio data and a brief review of the Diffusion Monte Carlo calculations of the zero-point energy. In section III properties of the PES, the characteristic stationary point geometries, dissociation features, and monomer properties beyond dissociation limit are presented. Diffusion Monte Carlo calculations are also presented as is a short molecular dynamics calculation of the branching ratio of CH_4D^+ to the two sets of products, $CH_3^+ + HD$ and $CH_2D^+ + H_2$. Finally, a summary and conclusions are given in section IV.

II. Methods and Calculation Details

A. Ab Initio Calculations. The previous PES we published[12,13] was obtained by fitting to MP2/cc-pVTZ ab initio data. The current fit uses a higher level of theory and larger basis set, CCSD(T)/aug-cc-pVTZ, for higher quality and a more accurate PES. For extending the PES to dissociation, many more ab initio points were obtained and they were created in several ways. First, geometries were directly taken from our previous calculations of the MP2-based PES. These were obtained using a combination of ab initio classical molecular dynamics ("direct-dynamics"), done at a lower level of ab initio theory and grids in normal coordinates.[12−14] Here we continued with this direct-dynamics approach but extended to higher total energies and supplemented those configurations with ones designed to focus on dissociation. Several direct-dynamics trajectories were done on very low theory/basis level which is MP2/cc-pVDZ but at higher given initial kinetic energy levels such as 10 500, 11 000, 11 500, and 12 000 cm^{-1} for obtaining part of additional geometries. Second, a dissociation coordinate, denoted *R*, which is the distance between the H_2 center of mass and the C atom of the CH_3^+, was used to obtain many additional configurations. Along this coordinate, which extended to 14.0 bohr, the potential was relaxed with respect to the remaining internal coordinates and the resulting path is our defined "dissociation minimum energy path".

The energy distribution of the ab initio data used in the fit (relative to the global minimum energy) is shown in Figure 1. As seen, most of the data set is at energies below 50 000 cm^{-1}, with a large concentration of energies below the dissociation energy of roughly 16 000 cm^{-1}. Energies much above that value come from repulsive configurations where bonds are compressed.

Finally, fits (described below) were done and redone based on using those additional configurations obtained from doing MD and quantum DMC calculations on preliminary fits.

B. Fitting the Potential Energy Surface. The earlier fitting procedures for CH_5^+,[12,14] and an early version of the $H_3O_2^-$ PES[23] are closely related to the one we describe in this paper. CH_5^+ has 12 vibrational degrees of freedom, however, to facilitate a description of the PES that is invariant with respect to a permutation of the five H atoms we use all 15 internuclear distances, as done previously.[12,14,23] The function describing the PES has the form[12]

$$V = p(x) + \sum_{i<j} q_{i,j}(x) y_{i,j} \tag{2}$$

where x is a 15-dimensional vector with components $x_{i,j} = \exp(-r_{i,j})$, $r_{i,j}$ is the distance between nuclei i and j, and $y_{i,j}$ is given by

$$y_{i,j} = \frac{e^{-r_{i,j}}}{r_{i,j}} \tag{3}$$

Here two functions p and q are used and they are seventh order and third-order multinomials of all $x_{i,j}$, respectively. In addition, p and q are constructed to satisfy the permutation symmetry with respect to the five hydrogen atoms.[12] Here we also introduce a "reaction coordinate" *R*, which is the distance between the carbon atom and the center of mass of the H_2 moiety. In the dissociation of CH_5^+ the complex dissociates to two fragments CH_3^+ and H_2. And *R* is large. Ab initio calculation of the super molecule, $CH_3^+ + H_2$, with the *R* large indicates that the potential of optimized CH_5^+ geometry will approach the dissociation energy D_e as R goes to infinity. In the current fit, $x_{i,j} = \exp(-r_{i,j})$ is used instead of $x_{i,j} = \ln(r_{i,j})$, which was used previously,[14] because the former can better describe the behavior of the potential in the dissociation region.

Some of the CCSD(T) energies were obtained at small C−H or H−H bond lengths where the potential is highly repulsive, cf. Figure 1. Thus, the fit used a weighted least squares approach such that geometries with energies above 30 000 cm^{-1} have a weight of 0.2 while those below 30 000 cm^{-1} have a weight of 1. The coefficients of the fit were computed using singular value decomposition.[24]

Finally, we extended the fit to properly describe the long-range electrostatic interaction, using a simple switching function[25] and an equation[26] describing the long range electrostatic interaction as described next.

C. Long-Range Interaction. As mentioned previously, the importance of reaction of $CH_3^+ + H_2$ motivated us to extend our PES to its dissociation region; in other words, CH_5^+ should be able to dissociate correctly to $CH_3^+ + H_2$ on our PES. We plan to use the PES for dynamics calculations of the reaction 1 at very low relative translational energies of relevance to astrochemistry. Thus, we are also concerned about having the correct long-range behavior of the interaction. Rather than extend the ab initio calculations and fit to very long range, we decided to smoothly join the current fit to the known long-range behavior of the interaction. This was done using the following expression:

$$V = V_{\text{fit}}[1 - S(R)] + S(R)V_{\text{LR}}; \quad 11 \le R \le 15$$
$$V_{\text{LR}} \equiv V_{\text{ion-induced dipole}} + V_{CH_3^+} + V_{H_2} + D_e \tag{4}$$

where $V_{fit}(R)$ is the potential energy obtained from the fit,

$V_{\text{ion-induced dipole}}$ is the analytically known long-range interaction, $V_{CH_3^+}$ and V_{H_2} are the potentials of these two monomers. D_e is the dissociation energy and $S(R)$ is a polynomial switching function that varies smoothly between 0 and 1 in a finite range.[25] S is given by

$$S(x) = \frac{a}{2}x^2 + \left(10 + \frac{b}{2} - \frac{3a}{2}\right)x^3 + \left(\frac{3a}{2} - b - 15\right)x^4 + \left(6 + \frac{b}{2} - \frac{a}{2}\right)x^5, \quad 0 \le x \le 1 \quad (5)$$

where $a = f''(0)$ and $b = f''(1)$, and in the present case a = $b = 0$ and $x = (R - R_{\min})/(R_{\max} - R_{\min})$. $V_{CH_3^+}$ and V_{H_2} were obtained from the CH_5^+ fit itself but at a large separation where the interaction is quite small (see below for more details). In eq 4, the long-range term $V_{\text{ion-induced dipole}}$ is given by the sum of charge-induced dipole (H_2), U_4 term[26]

$$U_4 = -\left[\frac{1}{2}\alpha + \frac{1}{3}(\alpha_{||} - \alpha_{\perp})P_2(\cos\theta)\right]/R^4 \quad (6)$$

and the charge-(H_2) quadrupole, U_3 term[26]

$$U_3 = Q_{H_2}P_2(\cos\theta)/R^3 \quad (7)$$

$$P_2(\cos\theta) = \frac{1}{2}(3\cos^2\theta - 1) \quad (8)$$

where θ is the angle between the vector $\boldsymbol{R}$ and the H_2 bond. α,$\alpha_{||}$ and $\alpha_{\perp}$ are the polarizabilities of the H_2 molecule, and Q_{H_2} is its quadrupole moment. α is the mean polarizability and given by[27]

$$\alpha = \frac{1}{3}(2\alpha_{\perp} + \alpha_{||}) \quad (9)$$

$\alpha_{||}$, $\alpha_{\perp}$, and Q_{H_2} were obtained using the cubic spline[28] interpolation based on the published polarizability data[29] and quadrupole moment data[30]

Finally, we have

$$V_{\text{ion-induced dipole}} = U_3 + U_4 \quad (10)$$

After some "experimentation", the switching range was chosen as $11 \le R \le 15$ bohr. Note that in this switching range the fragments are quite far apart and very weakly interacting. Further the fragments are semirigid molecules and thus it is not necessary for the long-range potential to be permutationally invariant.

D. Diffusion Monte Carlo calculations (DMC). The DMC method is a statistical way to solve the time-dependent Schrödinger equation in imaginary time. In the current calculation, we use the version originally developed by Anderson[31,32] and implemented by our collaborator McCoy.[33] The DMC calculations in this paper follow the approach described in detail elsewhere[12,13] for the MP2-based PES. Specifically in the notation of those papers $\alpha = 0.01$ hartree, the total propagation time = 10 000 time steps, with the time step = 10 au. Using these parameters we determined the zero-point energies (ZPEs) of CH_5^+ and selected isotopologs as well as the combined ZPEs of $CH_3^+ + H_2$ and selected isopologs.

III. Results and Discussion

A. Properties of the PES. Fitting Accuracy. The RMS fitting error vs $E_{\max}$ plot is presented in Figure 2 to show the accuracy of the PES. The error is 78.1 cm^{-1} for energies up to 30 000 cm^{-1}, which is roughly twice as the dissociation energy. Therefore, we are very confident that the fit will be accurate enough for both quantum and classical (or semiclassical) vibrational and scattering calculations.

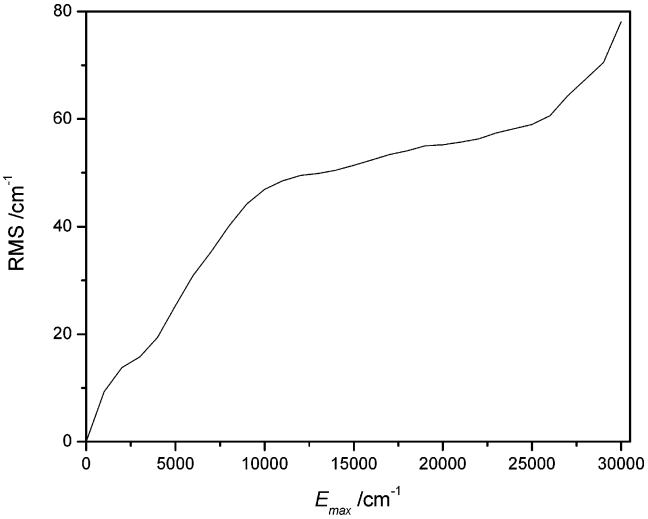

Figure 2. Fitting RMS error vs $E_{\max}$.

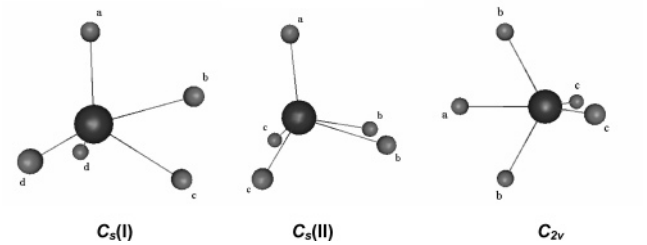

Figure 3. Representation of the three lowest energy stationary configurations of CH_5^+ from the PES. C_s(I) is the global minimum, C_s(II) is the lower energy saddle point, and C_{2v} is the higher energy saddle point. Atom labels are given to aid in locating the movement of atoms among these stationary points.

Stationary Point Analysis. The three stationary points of CH_5^+ are the minimum and two saddle points, denoted C_s(I), C_s(II), and C_{2v}, respectively. These were located on the PES using Newton's method. Considering the minimum as the reference energy, the energies of the C_s(II) and C_{2v} saddle points on the PES are 29.1 and 340.7 cm^{-1}, respectively; the corresponding ab initio values are 37.7 and 331.2 cm^{-1} at the geometries of the PES saddle points. The molecular geometries of these three stationary points are shown in Figure 3, using the notation of Schreiner et al.[5] The internuclear distances of these structures are given in Table 1 along with previous benchmark results of Schreiner et al.[5] As seen there is excellent agreement between the present PES and these benchmark calculations.

Next consider the normal-mode frequencies associated with these stationary points. These are given in Table 1. Because of the high computational cost, we carried out a direct ab initio normal-mode analysis at the minimum only. As seen there is very good agreement between the PES frequencies and the ab initio ones. The current frequencies are also close to those reported previously for the MP2-based PES.[14]

Fragment Properties. The current PES dissociates correctly to the fragments CH_3^+ and H_2. The minimum structure of CH_3^+ is planar as it should be with C−H bond lengths equal to 1.093 Å and the H_2 equilibrium bond length is 0.744 Å. These values compare very well with CCSD(T)/aug-cc-pVTZ ab initio calculations we did which give 1.091 and 0.743 Å, respectively.

TABLE 1: Geometry and Normal Mode Frequencies from the CH_5^+ Potential Energy Surface at the Minimum and Two Saddle Points, Denoted C_s(I), C_s(II), and C_{2v}, Respectively, with Comparisons with ab Initio Calculations Given

	C_s(I) (Å)	C_s(II) (Å)	C_{2v} (Å)
$C-H_a$	1.108 (1.106)[a]	1.084 (1.084)[a]	1.163 (1.162)[a]
$C-H_b$	1.197 (1.198)	1.200 (1.199)	1.087 (1.087)
$C-H_c$	1.197 (1.197)	1.100 (1.098)	1.142 (1.140)
$C-H_d$	1.088 (1.088)		
H_2	0.952 (0.945)	0.945 (0.940)	

mode	C_s(I) (cm^{-1})	C_s(II) (cm^{-1})	C_{2v} (cm^{-1})
1	199.9 (227.4)[b]	188.6i	698.5i
2	839.4 (831.3)	995.7	497.7
3	1296.7 (1284.3)	1151.2	1261.1
4	1303.5 (1291.2)	1340.3	1332.6
5	1477.7 (1464.1)	1482.1	1393.2
6	1499.9 (1492.9)	1507.1	1452.1
7	1586.7 (1595.8)	1603.2	1476.3
8	2417.9 (2430.1)	2401.1	2639.9
9	2707.7 (2714.9)	2728.8	2685.0
10	3001.0 (3011.0)	3037.8	2848.0
11	3132.9 (3130.2)	3090.5	3122.0
12	3224.4 (3224.4)	3236.1	3239.1

[a] Values in parentheses are CCSD(T)/TZ2P+*f* calculations of ref 5. [b] Values in parentheses are from present CCSD(T)/aug-cc-pVTZ ab initio calculations.

TABLE 2: Normal Mode Frequencies of CH_3^+ and H_2 from the CH_5^+ PES

mode	CH_3^+	H_2
1	1390.2 (1421.6)[a]	4377.0 (4400.2)
2	1412.1 (1429.0)	
3	1412.1 (1429.0)	
4	3031.2 (3039.3)	
5	3195.7 (3236.9)	
6	3195.7 (3236.9)	

[a] Numbers in parentheses are from present CCSD(T)/aug-cc-pVTZ calculations.

A normal-mode analysis was done on these fragments at a separation distance of $R = 14$ bohr and the results are given in Table 2. The result for H_2 is in excellent agreement with the benchmark value 4401 cm^{-1}. To compare the CH_3^+ frequencies with ab initio we computed the optimized structure and normal-mode frequencies using CCSD(T)/aug-cc-pVTZ calculations. These are also given in Table 2. Very good agreement is seen with the results from the present PES.

Behavior in the Switching Region. As noted the present PES is not designed to describe the long-range electrostatic interaction and thus the switching approach described above was taken. The main purpose of this enhancement to the PES is to describe the long-range interaction for use in dynamics calculations. The long-range electrostatic interaction (cf. eqs 4−10) depends on the orientation of H_2, θ, R, and also r_{HH}. The angular dependence of the combined potential in the switching region is shown in Figure 4, where $r_{HH} = r_e$ and CH_3^+ is also at equilibrium. At $R = 11$ bohr, the angular dependence is strictly from the PES, and at $R = 15$ bohr, it is from the added long-range potential. Obviously these two cannot be identical since they come from different sources; however, as seen the switch between the two is smooth even though there is larger angular dependence for the added potential than from the PES. The range of the angular variation is 20 cm^{-1} at 11 bohr, i.e., before the switching, and 80 cm^{-1} at 15 bohr, i.e., after the switching. These are small energies relative to the dissociation energy and they reflect the small differences in the long-range add-on to the PES and the PES itself. The dissociation energy D_e, obtained from the combined potential given by eq 4 obtained at $R = 100$ bohr is 16323 cm^{-1}. This compares very well with the value obtained form direct ab initio calculations at 100 bohr of 16321 cm^{-1}.

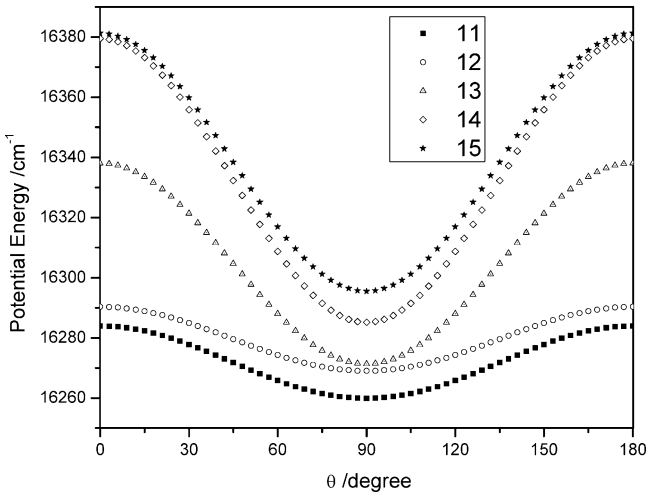

Figure 4. Angular dependence of potential energy on current PES within the switching region. The value in the legend is R, and the values are in bohrs and the angle θ is defined in the text.

TABLE 3: Zero Point Energies of CH_5^+ and Isotopologs

molecule	ZPE (cm^{-1})[a]
CH_5^+	10917 (3)
CH_4^+D	10300 (6)
$CH_3^+D_2$	9694 (3)
$CH_2^+D_3$	9097 (6)
CH^+D_4	8563 (3)
CD_5^+	8044 (2)

[a] Statistical uncertainty is in parentheses.

B. Diffusion Monte Carlo (DMC) Zero-Point Energies (ZPE) and D_0. To obtain D_0 for this floppy cation we calculated the ZPE of CH_5^+ and the separated fragments and combined those numbers with D_e in the usual way. Accurate ZPEs were obtained using DMC calculations described above and are given in Table 3. The results compare well, i.e., differ by 61 cm^{-1} or less, with those reported on the previous MP2-based PES[12,13] (which does not dissociate) for CH_5^+, $CH_2D_3^+$, and CD_5^+. Somewhat surprisingly the present ZPE for CH_5^+ is 177 cm^{-1} lower than ZPE reported by Thompson et al.[15] who reported a DMC calculation of the ZPE using an interpolated PES based on the same ab initio method and basis (CCSD(T)/aug-cc-pVTZ) used in the present work.

Since the present PES can correctly describe the dissociation we also performed DMC calculations of the ZPE of the fragments $CH_3^+ + H_2$ and the two sets of fragments of the CH_4D^+ dissociation, $CH_3^+ + HD$ and $CH_2D^+ + H_2$. These were done by separating the fragments and propagating using the full PES, as was done recently for the dissociation products of H_5^+, $H_3^+ + H_2$.[34] The energy is shown in Figure 5 vs the (imaginary) propagation time for $CH_3^+ + H_2$. As seen there is a plateau region corresponding to the ZPE of the combined but noninteracting fragments (relative to the potential minimum at CH_5^+), followed by a decline to another plateau corresponding to the ZPE of CH_5^+. From the ZPE calculations of the separated fragments and those of CH_5^+ and CH_4D^+ we obtain the following values of D_0: 14316 cm^{-1} for CH_5^+, 14650 cm^{-1} for CH_4D^+ to fragment to $CH_3^+ + HD$, and 14367 cm^{-1} to fragment to $CH_2D^+ + H_2$. Thus, the exoergicity of reaction 1

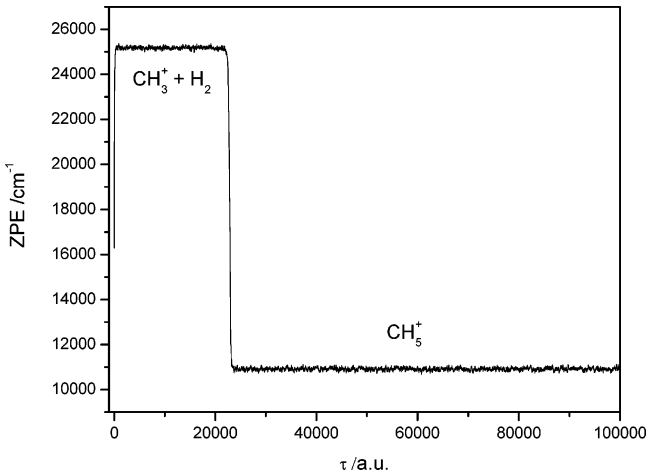

Figure 5. Energy vs (imaginary) time in DMC calculation of dissociated CH_5^+ fragment $CH_3^+ + H_2$.

is predicted to be 283 cm^{-1} which is (fortuitously) in nearly perfect agreement with a calculated estimate (including an empirical scaling factor) of 284 cm^{-1} [35] and the measured value of 260 cm^{-1}.[36] We estimate a conservative statistical uncertainty of ± 40 cm^{-1} in these values. The absolute uncertainty in the D_0s is certainly larger than the statistical uncertainly but is probably less than 100 cm^{-1}.

C. Molecular Dynamics Calculations of CH_4D^+ Dissociation. Finally we report a preliminary classical molecular dynamics simulation of the unimolecular CH_4D^+ dissociation to form the two possible products HD + CH_3^+ and H_2 + CH_2D^+. Of course any of the four H atoms can be found in the HD product, and the current potential does describe this multiplicity of products. The calculations were initiated at the global minimum with zero angular momentum and total energy of 25 000 cm^{-1}, which is roughly D_e plus the zero-point energies of the fragments. This energy was randomly distributed as kinetic energy among the internal modes and 1000 trajectories were done for each single site substitution of the five H atoms for a total of 5000 trajectories. Dissociation was reached when the separation between fragments, R, reached 10 bohr. The branching ratio from these trajectories is 0.65 for $H_2 + CH_2D^+$ and 0.35 for $HD+CH_3^+$ in very good agreement with the classical statistical prediction of 0.6 and 0.4. A more sophisticated approach with a better assessment of the probability distribution of the possible D atom sites will be done in the future (here we assumed equal probability). Also, an attempt to enforce the zero-point energies of the fragments should be done in a future calculation.

IV. Summary and Conclusions

In this paper, we presented a full-dimensional potential energy surface (PES) for CH_5^+ that dissociates to fragments $CH_3^+ + H_2$. We extended an approach used previously, which incorporates permutational symmetry into the fitting basis functions, by using a higher level of ab initio calculations, i.e., CCSD(T)/aug-cc-pVTZ and including more configurations to describe dissociation. Standard properties of the stationary configurations of the PES were shown to be in excellent agreement with previous benchmark calculations at these configurations. Properties of the CH_3^+ and H_2 fragments were also shown to be accurately obtained by the PES.

The analytical long-range ion-quadrupole and ion-induce dipole long-range behavior was added to the potential fit by means of a finite range switching function.

The PES was used in Diffusion Monte Carlo calculations of the zero-point energies of CH_5^+, deuterated isotopologs, and fragments. These together with the dissociation energy were used to predict D_0 for CH_5^+ and CH_4D^+. Finally a very brief molecular dynamics calculation of the product branching ratio of dissociation of CH_4D^+ at one energy and zero total angular momentum showed very good agreement with a simple classical statistical prediction.

Acknowledgment. The authors thank the National Science Foundation (CHE-0431998 and CHE-0443375) for financial support. Support for computational resources from an ONR/DURIP grant is also acknowledged. We thank Xinchuan Huang for useful discussions. The authors also thank Zhen Xie for useful discussions on geometry optimization code. The Diffusion Monte Carlo code we used is based on one kindly sent to us by Anne McCoy of The Ohio State University. We thank her for important advice on doing the Diffusion Monte Carlo calculations.

References and Notes

(1) Asvany, O.; Schlemmer, S.; Gerlich, D. *Astrophys. J.* **2004**, *617*, 685.
(2) Roberts, H.; Herbst, E.; Millar, T. J. *Astrophys. J.* **2003**, *591*, L41.
(3) Roberts, H.; Herbst, E.; Millar, T. J. *Mon. Not. R. Astron. Soc.* **2002**, *336*, 283.
(4) Schleyer, P. v. R.; Carneiro, J. W. D. *J. Comput. Chem.* **1992**, *13*, 997.
(5) Schreiner, P. R.; Kim, S. J.; Schaefer, H. F.; Schleyer, P. V. *J. Chem. Phys.* **1993**, *99*, 3716.
(6) Marx, D.; Parrinello, M. *Science* **1999**, *284*, 59.
(7) Marx, D.; Savin, A. *Angew. Chem., Int. Ed. Engl.* **1997**, *36*, 2077.
(8) Marx, D.; Parrinello, M. *Z. Phys. D: At. Mol. Clusters* **1997**, *41*, 253.
(9) Marx, D.; Parrinello, M. *Nature (London)* **1995**, *375*, 216.
(10) Schreiner, P. R. *Angew. Chem., Int. Ed.* **2000**, *39*, 3239.
(11) Müller, H.; Kutzelnigg, W.; Noga, J.; Klopper, W. *J. Chem. Phys.* **1997**, *106*, 1863.
(12) Brown, A.; McCoy, A. B.; Braams, B. J.; Jin, Z.; Bowman, J. M. *J. Chem. Phys.* **2004**, *121*, 4105.
(13) McCoy, A. B.; Braams, B. J.; Brown, A.; Huang, X. C.; Jin, Z.; Bowman, J. M. *J. Phys. Chem. A* **2004**, *108*, 4991.
(14) Brown, A.; Braams, B. J.; Christoffel, K.; Jin, Z.; Bowman, J. M. *J. Chem. Phys.* **2003**, *119*, 8790.
(15) Thompson, K. C.; Crittenden, D. L.; Jordan, M. J. T. *J. Am. Chem. Soc.* **2005**, *127*, 4954.
(16) Kaledin, A. L.; Kunikeev, S. D.; Taylor, H. S. *J. Phys. Chem. A* **2004**, *108*, 4995.
(17) Tal'roze, V. L.; Lyubimova, A. K. *Dokl. Bulg. Akad. Nauk. SSSR* **1952**, *86*, 909.
(18) Hiraoka, K.; Kebarle, P. *J. Am. Chem. Soc.* **1975**, *97*, 4179.
(19) Hiraoka, K.; Mori, T. *Chem. Phys. Lett.* **1989**, *161*, 111.
(20) White, E. T.; Tang, J.; Oka, T. *Science* **1999**, *284*, 135.
(21) Asvany, O.; Kumar, P.; Redlich, B.; Hegemann, I.; Schlemmer, S.; Marx, D. *Scienexpress* 2005.
(22) MOLPRO, a package of ab initio programs designed by Werner, H.-J.; Knowles, P. J., version 2002.6, with contributions from Amos, R. D.; Berhardsson, A.; Berning, A.; Schütz, M.; Lindh, R.; Celani, P.; Korona, T.; Rauhut, G.; Manby, F. R.; Cooper, D. L.; Deegan, M. J. O.; Dobbyn, A. J.; Eckert, F.; Hampel, C.; Hetzer, G.; Lloyd, A. W.; McNicholas, S. J.; Meyer, W.; Mura, M. E.; Nicklass, A.; Palmieri, P.; Pitzer, R.; Schumann, U.; Stoll, H.; Stone, A. J.; Tarroni, R.; Thorsteinsson, T. (Birmingham, U.K., 2002).
(23) Huang, X. C.; Braams, B. J.; Carter, S.; Bowman, J. M. *J. Am. Chem. Soc.* **2004**, *126*, 5042.
(24) Anderson, E.; Bai, Z.; Bischof, C.; et al. *LAPACK Users' Guide*, 3rd ed.; SIAM: Philadelphia, PA, 1999.
(25) Bowman, J. M.; Gazdy, B.; Schafer, P.; Heaven, M. C. *J. Phys. Chem.* **1990**, *94*, 2226.
(26) Prosmiti, R.; Buchachenko, A. A.; Villarreal, P.; Delgado-Barrio, G. *Theor. Chem. Acc.* **2001**, *106*, 426.
(27) Ishiguro, E.; Arai, T.; Mizushima, M.; Kotani, M. *Proc. Phys. Soc.* **1952**, *65A*, 178.
(28) Press, W. H.; Teukolsky, S. A.; Vetterling, W. T.; Flannery, B. P. *Numerical recipes in FORTRAN: the art of scientific computing*, 2nd ed.; Cambridge University Press: New York, 1992; Vol. 1.
(29) Kolos, W.; Wolniewicz, L. *J. Chem. Phys.* **1967**, *46*, 1426.

(30) Wolniewicz, L.; Simbotin, I.; Dalgarno, A. *Astrophys. J. Suppl. Ser.* **1998**, *115*, 293.
(31) Anderson, J. B. *J. Chem. Phys.* **1976**, *65*, 4121.
(32) Anderson, J. B. *J. Chem. Phys.* **1975**, *63*, 1499.
(33) McCoy, A. B. *Chem. Phys. Lett.* **2000**, *321*, 71.
(34) Xie, Z.; Braams, B. J.; Bowman, J. M. *J. Chem. Phys.* **2005**, *122*, 224307.
(35) Maluendes, S. A.; McLean, A. D.; Herbst, E. *Astrophys. J.* **1992**, *397*, 477.
(36) Smith, D.; Adams, N. G.; Alge, E. *Astrophys. J.* **1982**, *263*, 123.